



HAL
open science

Improving the performance of natural gas pipeline networks fuel consumption minimization problems

Firooz Tabkhi, Luc Pibouleau, Guillermo Hernandez-Rodriguez, Catherine Azzaro-Pantel, Serge Domenech

► **To cite this version:**

Firooz Tabkhi, Luc Pibouleau, Guillermo Hernandez-Rodriguez, Catherine Azzaro-Pantel, Serge Domenech. Improving the performance of natural gas pipeline networks fuel consumption minimization problems. *AICHE Journal*, 2010, 56 (4), pp.946-964. 10.1002/aic.12011 . hal-03474492

HAL Id: hal-03474492

<https://hal.science/hal-03474492>

Submitted on 10 Dec 2021

HAL is a multi-disciplinary open access archive for the deposit and dissemination of scientific research documents, whether they are published or not. The documents may come from teaching and research institutions in France or abroad, or from public or private research centers.

L'archive ouverte pluridisciplinaire **HAL**, est destinée au dépôt et à la diffusion de documents scientifiques de niveau recherche, publiés ou non, émanant des établissements d'enseignement et de recherche français ou étrangers, des laboratoires publics ou privés.



Open Archive Toulouse Archive Ouverte (OATAO)

OATAO is an open access repository that collects the work of Toulouse researchers and makes it freely available over the web where possible.

This is an author-deposited version published in: <http://oatao.univ-toulouse.fr/>
Eprints ID: 5000

To link to this article:

<http://dx.doi.org/10.1002/aic.12011>

To cite this version : Tabkhi, Firooz and Pibouleau, Luc and Hernandez-Rodriguez, G. and Azzaro-Pantel, Catherine and Domenech, Serge *Improving the performance of natural gas pipeline networks fuel consumption minimization problems*. (2010) AICHE Journal, vol. 56 (n° 4). pp. 946-964. ISSN 0001-1541

Any correspondence concerning this service should be sent to the repository administrator: staff-oatao@inp-toulouse.fr

Improving the Performance of Natural Gas Pipeline Networks Fuel Consumption Minimization Problems

F. Tabkhi, L. Pibouleau, G. Hernandez-Rodriguez, C. Azzaro-Pantel, and S. Domenech
Laboratoire de Génie Chimique-UMR 5503 CNRS/INP/UPS, 31106 Toulouse Cedex 1, France

As the gas industry has developed, gas pipeline networks have evolved over decades into very complex systems. A typical network today might consist of thousands of pipes, dozens of stations, and many other devices, such as valves and regulators. Inside each station, there can be several groups of compressor units of various vintages that were installed as the capacity of the system expanded. The compressor stations typically consume about 3–5% of the transported gas. It is estimated that the global optimization of operations can save considerably the fuel consumed by the stations. Hence, the problem of minimizing fuel cost is of great importance. Consequently, the objective is to operate a given compressor station or a set of compressor stations so that the total fuel consumption is reduced while maintaining the desired throughput in the line. Two case studies illustrate the proposed methodology. Case 1 was chosen for its simple and small-size design, developed for the sake of illustration. The implementation of the methodology is thoroughly presented and typical results are analyzed. Case 2 was submitted by the French Company Gaz de France. It is a more complex network containing several loops, supply nodes, and delivery points, referred as a multisupply multidelivery transmission network. The key points of implementation of an optimization framework are presented. The treatment of both case studies provides some guidelines for optimization of the operating performances of pipeline networks, according to the complexity of the involved problems.

Keywords: natural gas, network, pipeline, compressor, fuel consumption minimization, MINLP

Introduction

Natural gas, viewed as a cleaner-burning alternative to coal and oil in terms of acidic and greenhouse gas pollution, is increasingly being used as an energy source and by most valuations, its global consumption will double by 2030.¹ The transport of large quantities of natural gas is carried out by pipeline network systems across long distances. For example,

the European natural gas system, which is very well developed, consists of 1.4 million kilometers pipelines. As the gas flows through the network, pressure (and energy) is lost due to both friction between the gas and the pipe inner wall, and heat transfer between the gas and its environment. Typically, natural gas compressor stations are located at regular intervals along the pipeline to boost the pressure lost through the friction of the natural gas moving through the steel pipe. They consume a part of the transported gas, thus resulting in an important fuel consumption cost on the one hand, and in a significant contribution to CO₂ emissions, on the other hand.

Correspondence concerning this article should be addressed to L. Pibouleau at luc.pibouleau@ensiacet.fr

Thus, efficient operation of compressor stations is of major importance for enhancing the performance of the pipeline network. This article is devoted to the presentation of a systematic approach for optimizing the performance of compressor stations using a classical mathematical programming approach. Of course, several possible objective functions can be used to define the optimality of the network operation, as for instance, fuel consumption minimization, emission minimization, and pressure delivery satisfaction. For the two examples treated in this article, the total fuel consumption was selected as the unique objective function.

Indeed, as the gas industry has grown, gas pipeline networks have evolved over decades into very large and complex systems. A typical network today might consist of thousands of pipes, dozens of stations, and many other devices, such as valves and regulators. Inside each station, there can be several groups of compressor units of various vintages that were installed as the capacity of the system expanded. The compressor stations typically consume about 3–5% of the transported gas. It is estimated that the optimization of operations can significantly save the fuel consumed by the stations² even if only a local optimum is provided, compared with a nonoptimized solution.

Consequently, the objective is to operate each compressor station or a set of compressor stations so that the total fuel consumption is reduced while maintaining the desired throughput in the line. This problem is identified in the following part as compressor steady-state adjustment problem. Let us note that several requirements are imposed to the network, for instance, pressures at the endpoints of the network.

Two case studies illustrate the methodology and are presented in the following sections. The treatment of both case studies provides some guidelines for optimization of the operating performances of pipeline networks, according to the complexity of the involved problem.

Case study 1 involving a simple and small-size design is used as a test bench. The implementation of the methodology is thoroughly presented and typical results are analyzed.

Case study 2 was submitted by the French Company GdF Suez. It is a more complex network containing several loops, supply nodes, and delivery points, referred as a multisupply multidelivery transmission network.

Previous Works

Transmission pipeline modeling

Since 20 years, there has been an interest on the optimization of gas pipe distribution networks. Tian and Adewumi³ have proposed an one-dimensional compressible fluid flow equation. Lewandowski⁴ has implemented an object-oriented methodology for modeling a natural gas transmission network using a library of C⁺⁺ classes, and Osiadacz⁵ has presented a dynamic optimization of high-pressure gas networks using hierarchical system theory. Surry et al.⁶ have formulated the optimization problem based on a multiobjective genetic algorithm. Mohitpour et al.⁷ have used a dynamic simulation approach for the design and optimization of pipeline transmission systems. Boyd et al.⁸ have studied steady-state gas pipeline networks by modeling the compressor stations. Costa et al.⁹ have developed a steady-state gas

pipeline simulation. Sung¹⁰ have based their modeling approach on a hybrid network using minimum cost spanning tree. Sun et al.¹¹ have used a software support system called the Gas Pipeline Operation Advisor for minimizing the overall operating costs, subject to a set of constraints such as the horsepower requirement, availability of individual compressors, types of compressor, and the cycling of each compressor. A reduction technique for natural gas transmission network optimization problems was implemented by Rios-Mercado et al.¹² Martinez-Romero et al.¹³ have used the software package “Gas Net.” A MINLP model for the problem of minimizing the fuel consumption in a pipeline network was implemented by Cobos-Zaleta and Rios-Mercado.¹⁴ Mora and Uliuru¹⁵ have determined the pipeline operation configurations requiring the minimum amount of energy (e.g., fuel, power) needed to operate the equipment at compressor stations for given transportation requirements. Chauvelier-Alario et al.¹⁶ have developed CARPATHE, a simulation package (GdF Suez) for representing the behavior of multipressure networks and including functionalities for both network design and network operation. Optimization methods for planning reinforcement on gas transportation networks and for minimizing the investment cost of an existing gas transmission network were used by André et al.¹⁷

This literature analysis shows that there has been and continue to be a significant effort focused on the modeling of natural gas transmission networks. The objective of this work is to propose a general framework able to embed formulations from design to operational purposes: this explains why only steady-state behavior of the gas flow is considered. The problem is to implement, for a given mathematical model of a pipeline network, a numerical method that meets the criteria of accuracy together with relatively small computation times.

Optimization techniques

A large variety of applications, drawn from a wide range of investigation areas, can be formulated as complex optimization problems. As a consequence, a great diversity of optimization methods was implemented to meet the industrial stakes and provide competitive results. But if they prove to be well fitted to the particular case they consider, the numerical performances cannot be constant whatever the treated problem is. Actually, the efficiency of a given method for a particular example is hardly predictable, and the only certainty we have is expressed by the *No Free Lunch Theory*¹⁸: there is no method that outdoes all the other ones for any considered problem. This feature generates a common lack of explanation concerning the use of a method for the solution of a particular example. Among the diversity of optimization techniques, two important classes have to be distinguished: deterministic methods and stochastic ones. Complete reviews are proposed in literature for the two classes.^{19–21} A thorough analysis of both classes was previously studied by Ponsich²² with the support of batch plant design problems.

The deterministic methods assume the verification of mathematical properties of the objective function and constraints, such as continuity, differentiability, and convexity. In practice, these assumptions (particularly convexity) do not

always hold, and the convergence toward a global optimum is no longer guaranteed. This working mode enables only to ensure to get a local optimum, which is for all that a great advantage vs. stochastic methods. Among the deterministic class, particularly for NLP and MINLP problems considered in this study, the following procedures can be mentioned: the Outer Approximation algorithm,²³ the Branch & Bound methods for scanning trees,^{24–26} the Generalized Benders Decomposition,²⁷ the Extended Cutting Plane method for problems with a moderate degree of nonlinearity,²⁸ and disjunctive programming for quasi-convex problems.²⁹ Even though most of the aforementioned methods are only academic tools, some (either commercial or free) computational codes are available: the SBB, BARON, DICOPT++, and LOGMIP solvers within the GAMS modeling environment,³⁰ MINLP_BB,³¹ and α ECP.³² Concerning the global optimization of non convex problems, the interval analysis method^{33,34} is a promising tool, but restricted at the present time to small problems, due to very high computational times.

The second class, namely, stochastic methods, is based on the evaluation of the objective function at different points of the search space. These points are chosen through a set of heuristics, combined with generations of random numbers. Thus, stochastic procedures cannot guarantee to obtain an optimum. They are divided into neighborhood techniques such as Simulated Annealing,³⁵ Tabu Search,³⁶ and evolutionary algorithms comprising genetic algorithms,³⁷ evolutionary strategies,³⁸ and evolutionary programming.³⁹ Even if stochastic methods do not require any mathematical property for the objective function and constraints, they are difficult to implement for problems involving a significant number of equality constraints because the points chosen according heuristics or generated through genetic operators must verify the constraints.

As the number of equality constraints associated with the formulation of the problem related to the optimization of natural gas transmission networks may be important, the stochastic approach seems to be inefficient for this study. Within the deterministic class, solvers of the GAMS environment were chosen, as this optimization package is widely used, and even stands as a reference for the solution of problems coming from Process Engineering. From the numerical study of Ponsich,²² the MINLP problem will be solved by means of SBB whereas the NLP solver used with SBB being CONOPT. For the pure NLP problem, CONOPT is also used.

Modeling gas pipeline networks

Gas Pipeline Equations. The governing equation giving the pressure at each point of a straight pipe can be derived as follows:

$$\frac{dP}{dx} + \frac{f\rho\bar{v}^2}{2D} + \frac{d(\rho\bar{v}^2)}{dx} = 0 \quad (1)$$

where ρ is the gas density (kg/m³), D the pipe diameter, and \bar{v} the average gas velocity (m/s).

This relationship is obtained from the one-dimensional momentum balance around a horizontal cylindrical control

volume in steady state behavior. The Darcy friction factor, f , is a dimensionless value that is a function of the Reynolds number, Re , and relative roughness of the pipeline, ϵ/D . The Darcy friction factor is numerically equal to four times of the Fanning friction factor that is preferred by some engineers.

Since the regime of the gas passing through pipelines lies in the turbulent range, it is assumed that the wall roughness is the limiting factor compared with the Reynolds number to find out the value of the friction factor. The work of Romeo et al.⁴⁰ is used to estimate the friction factor. The momentum balance in terms of pressure and throughput can be written in the following form:

$$\frac{dP}{dx} + \frac{8fZRTm^2}{\pi^2MD^5P} + \frac{16Rm^2}{\pi^2MD^4} \frac{d}{dx} \left(\frac{ZT}{P} \right) = 0 \quad (2)$$

In this equation, Z is the compressibility factor, R is the universal gas constant [8314 J/(kmol K)], T is the temperature (K), M is the average molecular mass of the gas, and m is the pipe throughput (flow rate in kg/s).

By integrating Eq. 2 between two points i and j , the following equation is obtained and will be used in the numerical formulations. By assuming a constant temperature and constant compressibility factor between the integration points, the following expression is obtained:

$$P_i^2 - P_j^2 - \frac{32ZRTm^2}{\pi^2MD^4} \ln\left(\frac{P_i}{P_j}\right) + \frac{16fZRTm^2L}{\pi^2MD^5} = 0 \quad (3)$$

where L (m) is the pipe length between points i and j .

This relationship between pressure and flow rate exhibits a high degree of nonlinearity. It evaluates the pressure drop corresponding to a given flow magnitude and direction. This equation is used to estimate the pipeline's pressure profile and can incorporate the pressure head that occurs due to the location of the pipeline via the elevation changes.

The compressibility factor, Z , is used to alter the ideal gas equation to account for the real gas behavior. Traditionally, the compressibility factor is calculated using an equation of state. Yet, for natural gas, it may be estimated from the empirical relationship proposed for simulation goals in the literature.⁴¹ For example, this factor can be expressed as a function of the critical properties of the gas mixture, average pressure of the pipe segment, and the temperature that have been considered as constant:

$$Z = 1 + \left(0.257 - 0.533 \frac{T_c}{T} \right) \frac{P_{ij}}{p_c} \quad (4)$$

$$T_c = \sum T_{ci}y_i \quad (5)$$

$$p_c = \sum p_{ci}y_i \quad (6)$$

The pseudocritical temperature of natural gas, T_c , and its pseudo critical pressure, p_c , can be calculated using an adequate mixing rule starting from the critical properties of the natural gas components. The critical point of a

component is the point in which the distinction between the liquid and vapor phases disappears. In this work, average pseudocritical properties of the gas are determined from the given mole fractions of its components by Kay's rule which is a simple linear mixing rule shown in Eqs. 5 and 6.

Then average pressure, p_{ij} , can be calculated from two end pressures⁴¹:

$$p_{ij} = \frac{2}{3} \left(p_i + p_j - \frac{p_i p_j}{p_i + p_j} \right) \quad (7)$$

Maximum allowable operational pressure

The internal pressure in a pipe causes the pipe wall to be stressed, and if allowed to reach the yield strength of the pipe material, it could cause permanent deformation of the pipe and ultimate failure. In addition to the internal pressure due to gas flowing through the pipe, the pipe might also be subjected to external pressure which can result from the weight of the soil above the pipe in a buried pipeline, and also by the probable loads transmitted from vehicular traffic. The pressure at all points of the pipeline should be less than the maximum allowable operating pressure (MAOP) which is a design parameter in the pipeline engineering. This upper limit is calculated using Eq. 9, where t is the thickness of the pipe⁴²:

$$p < \text{MAOP} \quad (8)$$

$$\text{MAOP} = \text{SMYS} \frac{2t}{D - t} f_F f_E f_T \quad (9)$$

The yield stress used in Eq. 9, is called the specified minimum yield strength (SMYS) of pipe material. SMYS is a mechanical property of the construction material of the gas pipeline. The factor f_F has been named the design factor. This factor is usually 0.72 for cross-country or offshore gas pipelines, but can be as low as 0.4, depending on class location and type of construction. The class location, in turn, depends on the population density in the vicinity of the pipeline. The seam joint factor, f_E , varies with the type of pipe material and joint type. Seam joint factors are between 1 and 0.6 for the most commonly used material types. The temperature factor, f_T , is equal to 1 for the gas temperature below 393 K but it can reach 0.867 at 503 K. For each particular problem, these factors are well known by the natural gas practitioners.

Critical velocities

The gas velocity is directly related to the flow rate. As flow rate increases due to the augmentation in pressure drop, so does the gas velocity. An important factor in the treatment of compressible fluid flow is the so-called critical flow. For a compressible flow, the increase in flow owing to the pressure drop increase is limited to the velocity of sound in the fluid, i.e., the critical velocity. Sonic or critical velocity is the maximum velocity which a compressible fluid can reach in a pipe. For trouble-free operation, velocities maintain under a half of sonic velocity. The sonic velocity in a

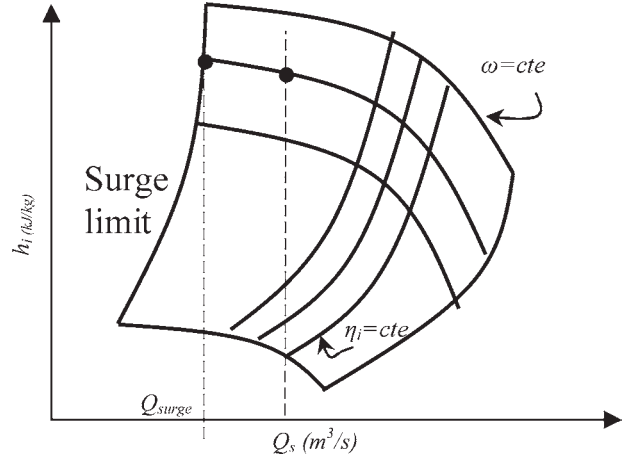


Figure 1. A typical centrifugal compressor map.

gas, c is calculated using Eq. 11, where κ is the average isentropic exponent of the gas and C_p is the heat capacity at constant pressure in J/(kmol K).

$$v < c/2 \quad (10)$$

$$c = \sqrt{\frac{\kappa ZRT}{M}} \quad (11)$$

$$\kappa = \frac{\sum C_{p,i} y_i}{M \sum (C_{p,i} y_i) - R} \quad (12)$$

Increasing gas velocity in a pipeline can have a particular effect on the level of vibration and increase the noises too. Moreover, higher velocities in the course of a long period of time will cause the erosion of the internal surface of the tubes, elbows, and other joints. The upper limit of the velocity range should be such that erosion–corrosion cavitations or impingement attack will be minimal. The upper limit of the gas velocity for the design purposes is usually computed empirically with the following equation.⁴² In pipeline design domain, the erosional velocity v_e must always be less than the speed of sound in the gas.

$$v < v_e \quad (13)$$

$$v_e = 122 \sqrt{\frac{ZRT}{PM}} \quad (14)$$

Compressor characteristics

As shown in Figure 1, a centrifugal gas compressor is characterized by means of its delivered flow rate and its pressure ratio, the ratio between suction side pressure of the compressor and its discharge pressure. The compression process in a centrifugal compressor can be well formulated using isentropic process aiming for calculating horsepower for a compressor station. The pressure ratio of a centrifugal compressor is usually linked with a specific term named “head” carried over from pump design nomenclature and expressed in meter even for compressors. The “head”

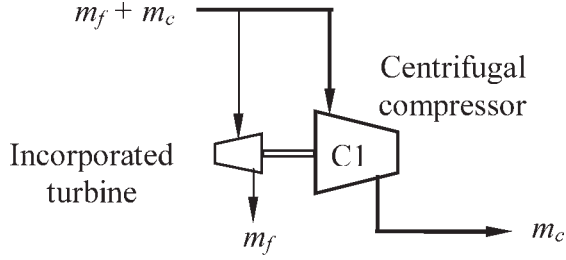


Figure 2. Representation of the centrifugal compressor and its incorporated turbine.

developed by the compressor is defined as the amount of energy supplied to the gas per unit mass of gas.

The equation for power calculation can be expressed as follows:

$$P_w = \frac{m_c h_i}{\eta_i} \quad (15)$$

where m_c (kg/s) is the mass flow rate of compressed gas, h_i (m) is the compressor isentropic head, and η_i is the compressor isentropic efficiency.

For adiabatic compressor the adiabatic efficiency is defined by:

$$\eta_i = \frac{P_{w,ideal}}{P_w} \quad (16)$$

As shown in the following equation, considering adiabatic compression, head is an index of the pressure ratio across the compressor. In this equation, p_d is the discharge pressure of the compressor, p_s is the suction pressure, and κ is the isentropic exponent and will be calculated using Eq. 12. The compressibility factor and the temperature here are considered at suction side of the compressor, where M is the average molecular mass of the gas.⁴³

$$h_i = \frac{Z_s R T_s}{M} \frac{\kappa}{\kappa - 1} \left[\left(\frac{p_d}{p_s} \right)^{\frac{\kappa - 1}{\kappa}} - 1 \right] \quad (17)$$

Centrifugal compressors in the station are assumed to be driven by turbines whose supply energy is provided from a line of the gas derived from the pipeline passed through the station to be compressed as shown in Figure 2. The flow rate of the consumed gas as fuel for the compression process in each compressor is obtained by dividing required power for compression, P_w , by the mechanical efficiency, η_m , driver efficiency, η_d , and LHV (low heating value):

$$m_f = \frac{10^6 m_c h_i}{\eta_i \eta_m \eta_d \text{LHV}} \quad (18)$$

LHV represents the quantity of energy released by mass unity of the gas during complete combustion. It is considered at 298 K and 1 bar in (kJ/kg) and is calculated from the mass lower heating values, LHV_i of the molecules composing the gas (M_i is the molecular mass of specie i):

$$\text{LHV} = \frac{\sum y_i M_i \text{LHV}_i}{\sum y_i M_i} \quad (19)$$

The adiabatic efficiency η_i is defined by Eq. 21 for the first numerical example and for the second it was fixed by GdF Suez at 0.75 for all the compression stations. For the compressor adjustment problem, we have $\eta_m = 0.90$ and $\eta_d = 0.35$,⁴⁴ whereas for the multisupply multidelivery transmission network, GdF suggests $\eta_m \times \eta_d = 0.35$.

Applying standard polynomial curve-fitting procedures for each compressor, the normalized head h_i/ω^2 can thus be obtained under the form of the following equation.⁴⁴

$$\frac{h_i}{\omega^2} = b_1 + b_2 \frac{Q_s}{\omega} + b_3 \left(\frac{Q_s}{\omega} \right)^2 \quad (20)$$

where Q_s is the volumetric flow rate (m³/s).

In the same way, contours of constant isentropic efficiency could be fitted in the polynomial form of second degree shown in Eq. 21:

$$\eta_i = b_4 + b_5 \frac{Q_s}{\omega} + b_6 \left(\frac{Q_s}{\omega} \right)^2 \quad (21)$$

The rotational speed ω (defined from Eqs. 17 and 20) of all compressors is comprised between lower and upper bound as represented below. To prevent from surge phenomenon, by considering a surge margin, λ_{surge} , the following constraint is introduced⁴⁵:

$$\omega_l \leq \omega \leq \omega_u \quad (22)$$

$$\lambda_{\text{surge}} \leq \frac{Q_s - Q_{\text{surge}}}{Q_s} \quad (23)$$

There is a surge flow rate, Q_{surge} , corresponding to each compressor rotational speed⁴⁶:

$$Q_{\text{surge}} = b_1 \left(\left(\frac{Z_s R T_s \kappa - 1}{M p_s^2 \kappa} h_{\text{surge}} + \left(\frac{Z_s R T_s}{p_s M} \right)^2 \right)^{\frac{\kappa}{\kappa - 1}} - \left(\frac{Z_s R T_s}{p_s M} \right)^2 \right)^{1/2} \quad (24)$$

In this equation, h_{surge} is the surge head at a specified compressor speed and can be calculated using following equation:

$$\frac{h_{\text{surge}}}{\omega^2} = b_1 + b_2 \frac{Q_{\text{surge}}}{\omega} + b_3 \left(\frac{Q_{\text{surge}}}{\omega} \right)^2 \quad (25)$$

Considering a fixed value for a given surge efficiency, the surge efficiency will be introduced as a parameter during the optimization procedure. Previous equation represents a non-linear correlation between surge flow rate and rotational speed of the compressor.

To avoid choking occurrence at inlet, the following inequality should be considered.

$$Q_s \leq A_s c \left[\frac{2}{\kappa + 1} \right]^{\frac{\kappa+1}{2(\kappa-1)}} \quad (26)$$

In this inequality, A_s is the cross-sectional area and c_s is the gas sonic velocity at the compressor inlet. Another inequality is introduced corresponding to the protection of a compressor against choking phenomenon in impeller passages as shown in Inequality (27). In this expression, the impeller radius, r in m and A , the flow rate area in m^2 are considered at the section of rotating passages as well as Q , Z , T , p . The Index 1 indicates the impeller inlet state.

$$Q \leq \frac{ZRT}{pM} \rho_1 c_1 A \left[\frac{2 + (\kappa - 1)(r\omega)^2 / c_{01}^2}{\kappa + 1} \right]^{\frac{\kappa+1}{2(\kappa-1)}} \quad (27)$$

To stay away from diffuser choking, another inequality similar to that of the compressor inlet is considered, but as shown below, in this relation the gas properties are in the conditions of the diffuser and Index 2 is used for diffuser inlet. The derivations of these three latter inequalities are presented in literature.⁴⁷ It is clear that the conditions at diffuser inlet are dependent on the impeller process, thus:

$$Q_f \leq \frac{Z_f RT_f}{p_f M} \rho_{02} c_{02} A_f \left[\frac{2}{\kappa + 1} \right]^{\frac{\kappa+1}{2(\kappa-1)}} \quad (28)$$

Representing network topology by using incidence matrices

The different links between the elementary sections of a network can be defined using incidence matrices. So, all the relation between the variables of the system such as the material balances at steady state around the nodes of a pipeline network can be expressed under a very concise form by using different types of incidence matrices such as the arc-node matrix.² In the model, each pipe, each compressor, and each fuel stream are represented by an arc. Consider a network with N_n nodes, N_p pipe arcs, and N_c compressor arcs. Therefore, there will be N_c fuel streams as for each compressor unit there is a stream that carries fuel to it. Because in a compressor, compression process is carried out, a compressor unit can be named an active arc. In this way, a pipe segment, in which the pressure decreases, may be called a passive arc. Let us note that the fuel streams have been considered as inert arcs regarding pressure change through them. A flow direction is assigned preliminarily to each pipe that can or not coincide with the real flow direction of the gas that running through the arc. N_v valves can be introduced into the network to break the pressure between some pairs of arcs to balance the network.

Let A be a matrix of dimension $N_n \times (N_p + N_c + N_v)$, where each of its elements, a_{ij} , is given the following attribution:

$$a_{ij} = \begin{cases} 1 & \text{if arc } j \text{ comes out from node } i \\ -1 & \text{if arc } j \text{ goes into node } i \\ 0 & \text{otherwise} \end{cases} \quad (29)$$

A is called the node-arc incidence matrix. Similarly, let B be another matrix of dimension $N_p \times N_c$ whose elements, b_{ij} , are defined below and it is named the pipe-compressor incidence matrix:

$$b_{ij} = \begin{cases} 1 & \text{if pipe } i \text{ is connected to discharge node} \\ & \text{of compressor } j \\ -1 & \text{if pipe } i \text{ is connected to suction node} \\ & \text{of compressor } j \\ 0 & \text{otherwise} \end{cases} \quad (30)$$

The last matrix is the node-fuel incidence matrix which describes the existing fuel stream derivations from a node and it is called the compressor-fuel matrix. The dimension of this matrix is $N_n \times N_c$ and its elements are defined below:

$$c_{ij} = \begin{cases} 1 & \text{if fuel stream } i \text{ be derived from node } j \\ 0 & \text{otherwise} \end{cases} \quad (31)$$

This matrix indicates which fuel stream belongs to which compressor.

These three incidence matrices are used to write the material balances around each node i , the flow rate of the consumed gas as fuel for the compression process in each compressor, and the equation of movement. For example, the material balance around the node i is expressed as Eq. 32. In this equation, S_i represents the gas delivery or supply relative to this node. It is negative if the node is a delivery one and positive for a supply node where the gas is injected to the node.

$$\sum_{j \in \text{arcs}} a_{i,j} m_j + \sum_{j \in \text{compressors}} b_{i,j} m_{f_j} = S_i \quad (32)$$

MINLP Formulation

Network characteristics

The MINLP formulation of a multisupply multidelivery transmission network is presented in this section. The system is composed of D_p delivery points at which gas comes out from the network. In the two following examples, these delivery points are symbolized by small empty circles. Gas can be supplied from S_p supply points symbolized by hexagons. Moreover, I_n intermediate nodes are considered to provide necessary interconnections or, in some cases, to specify explicitly some changes in design parameters: for example, some nodes are introduced for modeling the diameter change between two arcs (Node 103 in Figure 5), or when the pressure limits are different at the endpoints of their neighboring arcs (Node 66 in Figure 5). Globally, the network consists of N_n nodes and N_p pipe arcs. In addition, N_c compressors are located in the network to compensate for pressure losses. N_v

Table 1. Coefficients of the Isentropic Head Equation and Coefficients of the Isentropic Efficiency Equation of the Compressors

Coefficient	b_1	b_2	b_3	b_4	b_5	b_6
Value	3.8113×10^{-4}	3.849×10^{-6}	-6.3985×10^{-9}	17.269	0.3237	-4.1789×10^{-6}
Unit	m^2	m^{-1}	m^{-4}	–	m^{-3}	m^{-6}

valves permit to break the pressure between some pairs of points to balance the network. In some cases, a valve or more can be positioned after a compressor to regulate the output pressure of two or more streams that originate from the discharge side of compressor.

This node-arc incidence matrix has a dimension of $N_n \times (N_p + N_c + N_v)$ and is used in the problem formulation step. Let us recall that the term $a_{i,j}$ is equal to (+1) if downstream node of arc j is node i and is equal to (–1) if its upstream node is node i . Upstream and downstream assignments have been proposed by implementation of a rough free-hand material balance calculation around the nodes, with flow rate assumptions concerning few arcs.

The other data on the network are the following:

- (1) Pressure bounds for each node.
- (2) Characteristics of pipe arcs (length, internal diameter, inner surface roughness, MAOP).
- (3) Amount of gas delivery at each internal node.
- (4) Maximum amount of gas provided by the supply nodes.
- (5) Compressor characteristics, MAOP, capacity, maximum pressure ratio, maximum power.
- (6) Natural gas composition and thermodynamic properties.

Problem formulation

To tackle the problem, flow directions for each pipe arc as well as for each compressor and valve arc are not imposed in advance. Let us note that some particular cases, arc directions can be considered as fixed without any ambiguity during the optimization process (see Example 2). For each other arc, a binary variable d_i is assigned to identify its flow direction. This binary can be 0 or 1: when it is equal to 0, the gas flows in the arc opposite to the preliminary direction which is the direction conform to the corresponding node-arc incidence matrix used for initializing the search. The mixed integer nonlinear problem is formulated as below.

The continuous variables are pressures at nodes and flow rates corresponding to pipes, valves, and compressors, in addition to the gas injection flow rates at supply nodes, they all take positive values. The rotational speeds of the compressors have not been explicitly considered as variables, as the flow rates of the fuel streams have already been considered as variables for each compressor. As shown in Eqs. 18–25, the rotational speeds are directly dependent on the fuel stream flow rates. The coefficients b_i of Eqs. 20 and 21 are reported in Table 1.

The equality constraints are related to the following: mass balances around nodes, equation of motion for each pipe arc (Eqs. 3–7), equations for compressors (power, efficiency, isentropic head, Eqs. 15–17), relationships between rotational

speed, suction volumetric flow rate of the consumed gas, and head of each compressor (Eqs. 18–20), and isentropic efficiency (Eq. 21), fuel consumption calculation at each compressor. Moreover, the involved inequality constraints are: a lower bound for delivery flow rate, an upper bound as well as a lower bound for the pressures of the nodes, MAOP as an upper bound (for the first example, the following values were chosen for computing the MAOP: $f_F = 0.72$, $f_E = 1$, $f_T = 1$; for the second example, the values of MAOP were directly provided by GdF Suez, see Tables 8 and 12) and atmosphere pressure as a lower bound (Eq. 9), half the speed of sound and erosional velocity in the role of upper bounds of the velocities through pipes (Eqs. 10–14), lower and upper bounds on the rotation speed of all compressors (Eq. 22), a lower bound on compressor throughput taken to avoid pumping phenomenon (Eqs. 23–25), an upper bound on compressor throughput to prevent from choking phenomenon (Eqs. 26–28).

For each valve, there is a relationship in the form of a mixed inequality. The constraint related to a valve is considered as a linear inequality satisfying just that the downstream pressure is lower than or equal to the upstream pressure:

$$\sum_i P_i(2d_j - 1)a_{ij} \geq 0 \quad j \in N_v \quad i \in N_n \quad (33)$$

In this equation, p_i refers to the pressure, d_j is a binary used to define flow direction through valve, and a_{ij} 's are the components of the node-arc incidence matrix A corresponding to the associated valve. Note that this equation introduces bilinearities between variables and may give birth to several local solutions. This is the reason why several initial points are used in the second example.

The total sum of the fuel consumption in compressors is the objective function, as expressed in Eq. 34. For each compressor, fuel consumption flow rate, $m_{f,i}$, is obtained by using Eq. 18.

$$f_{\text{obj}} = \sum_{i \in \text{compressors}} m_{f,i} \quad (34)$$

First numerical example: compressor adjustment problem (NLP problem)

Network Characteristics. The first example is inspired from the work of Abbaspour et al.⁴⁴ (see Figure 3). The network consists of three long pipelines of 100 km. There are two compressor stations that operate to compensate for pressure drop in the pipelines. Each compressor station includes three parallel centrifugal compressors. In each station, there are six short pipe segments of about a hundred meters linked

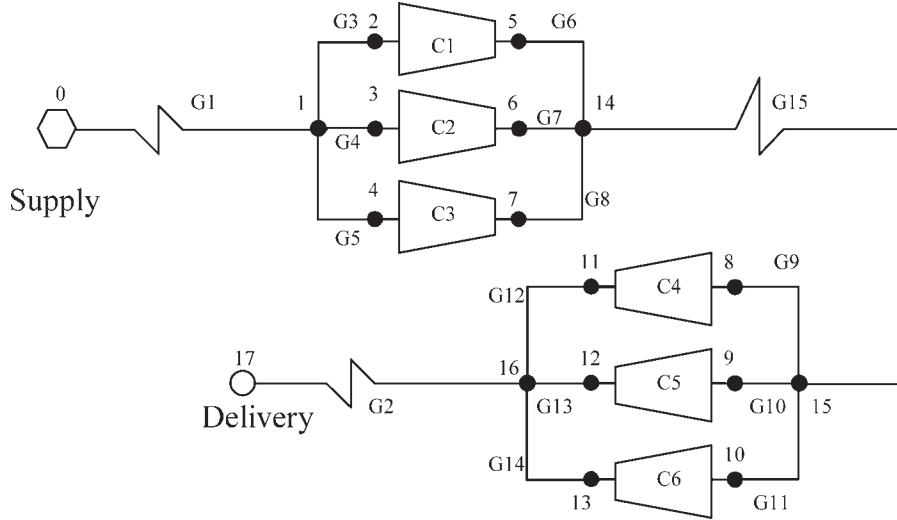


Figure 3. Schema of the considered pipeline network in case study 1.

to the entrances and outlets of the compressors. Although the length and the diameter of these pipes is lower than those of the three major pipelines, their role in the pressure change through the network may not be negligible and may even sometimes become bottleneck of the system. Therefore, these pipelines are also considered in the model. The technical features of the pipeline system corresponding to Figure 3, considered as fixed parameters for the optimization problem, are proposed in Table 2.

The pressure is considered to be equal to 60 bars with a margin of $\pm 2\%$ at the entrance point of the network, Node 0, as well as the delivery pressure, at Node 17 (in other words the lower bound is 58.8 bar and the upper one is 61.2 bar). The gas flows from Node 0 toward Node 17, and there is no input or output in the other nodes. The typical composition of natural gas considered in the numerical runs is presented in Table 3 with also the thermodynamic properties of gas components. Roughness of inner surface of the pipes is considered to be equal to 46×10^{-6} (traditional value reported for stainless steel). The temperature is assumed to be isothermal and equal to 330 K all over the system. The adiabatic efficiency η_i is defined by Eq. 21, and mechanical efficiency and driver efficiency for the compressors are assumed to be 0.90 and 0.35, respectively, according to values proposed in the dedicated literature.⁴²

The network includes 18 nodes, 15 pipes arcs, and six compressor arcs. As for each compressor unit, there is a stream that carries fuel to it; there are six fuel streams which have not been shown in Figure 3 to avoid complexity. For each compressor, this stream originates from suction node. A flow direction is assigned to each pipe so the gas flows from 0 to 17. So, the integer variables d_i related to flow directions

disappear from the original MINLP problem, which is reduced here to a NLP one.

For example, the node-arc incidence matrix, named A (see Figure 4) is a matrix of dimension $18 \times (15 + 6)$ (the network does not involve any valve). The material balance around the nodes can be stated in a very concise way by using this matrix.

NLP Formulation. The continuous variables of this problem are as follows: 18 pressure variables governing the nodes and 21 flow rate variables (including fuel streams) corresponding to pipes and compressors. The equality constraints consist of 18 mass balances around nodes, 15 equations of motion for the pipe arcs, six isentropic head equations for compressors as shown in Eq. 17, six relationships between rotational speed, suction volumetric flow rate, and head of each compressor (Eq. 20), six equations to calculate isentropic efficiency according to Eq. 21, and six equations to determine fuel consumption at each compressor unit. The set of inequality constraints is constituted by a lower bound for delivery flow rate (flow rate in arc G2) equal to 150 kg/s, an upper bound as well as a lower bound for the pressures of the nodes (MAOP as an upper bound and atmosphere pressure as a lower bound), sonic velocity and erosional velocity in the role of upper bounds of the velocities through pipes, lower and upper bounds on the rotation speed of all compressors (166.7 and 250 rpm, respectively), a lower bound on compressor throughput to avoid pumping phenomenon, an upper bound on compressor throughput to prevent from chocking phenomenon. In total, there are 57 equality constraints and 76 inequality constraints. The objective function to be minimized is given by Eq. 34.

Table 2. Technical Features of the Pipelines of the System Shown in Figure 3

Pipeline Tag	G1	G2	G3	G4	G5	G6	G7	G8	G9	G10	G11	G12	G13	G14	G15
Diameter (m)	0.787	0.889	0.330	0.381	0.330	0.330	0.330	0.330	0.381	0.330	0.432	0.330	0.330	0.330	0.838
Length (m)	1E + 5	1E + 5	200	300	100	200	100	200	100	100	100	100	400	100	1E + 5

Table 3. Parameters of the Optimization Problem Related to the Components of Gas Flowing in the Pipeline of Case Study 1

Component	Methane	Ethane	Propane
Mole percent	70	25	5
Molecular weight	16.04	30.07	44.1
Critical temperature, K	190.6	305.4	369.8
Critical pressure, bar	46	48.8	42.5
Lower heating VALUE, (kJ/kg)	50009	47794	46357
Heat capacity at constant pressure, (kJ/(kmol K))	35.663	52.848	74.916

Problem Solution. The initialization of the variables is performed directly through the software (GAMS/CONOPT) under the condition that the problem is well-scaled and that bounds are assigned adequately. For bounded variables, GAMS takes the initial values in the middle of the bounds. Several other initial points were randomly selected (inside the bounds, for bounded variables), the same solution was obtained. Strictly considering the nonconvexity feature, the example is not so strongly nonconvex.

The options used for implementing CONOPT are as follows: optimality tolerance = 10^{-8} , maximum feasibility tolerance = 10^{-5} , number of stalled iterations = 100. The resolution takes about 0.5 s CPU on a PC (processor Celeron 2.53 MHz, RAM 224 Mo). Table 4 presents the results relative to pressure value at each node. Observe that at Node 0 (i.e., supply node), the algorithm has taken the maximum possible pressure (61.2 bar) whereas the minimum possible

value (58.8 bar) was obtained at Node 17 (i.e., delivery node).

The value of objective function that is the total fuel consumption in the compressor stations is equal to 0.749 kg/s (sum of individual compressor consumptions, see Table 6) which leads to a significant reduction of 15% from the initial solution (0.863 kg/s (for initial value between their bounds), which represents a viable solution for the practitioner. The values of the optimal flow rates through pipelines are presented in Table 5. The optimum percentage of the input gas that is consumed in the stations can thus be calculated and is found equal to 0.497%. Additional information concerning compressor operating conditions can be deduced from pressure and flow rate optimal values (see Table 6): discharge flow rate, rotational speed, consumption ratio, isentropic head, isentropic efficiency, and individual fuel consumption of course. For each compressor, consumption ratio is defined as the fuel consumption divided by the input mass flow rate.

Let us mention in this example that the compressors involved in the second station work at their minimum rotational speeds, whereas the compressors of the first station work close to their maximum speeds. Finally, the transmitted power of the pipeline, that is the product of the pipeline delivery throughput (150 kg/s) and the lower heating value (LHV) of the natural gas (48,830 kJ/kg), is found to be equal to 7324 MW at this optimal point.

We may, therefore, conclude that in this example, network optimization is a viable alternative to find adequate operating conditions for pipeline network and this low-size example provides encouraging results. The methodology is now applied to a larger network, to illustrate the capability of the approach and to treat real problems involving a great number of variables.

Arc:	G1	G2	G3	G4	G5	G6	G7	G8	G9	G10	G11	G12	G13	G14	G15	C1	C2	C3	C4	C5	C6	Node:	
A =	+1	0	0	0	0	0	0	0	0	0	0	0	0	0	0	0	0	0	0	0	0	0	0
	-1	0	+1	+1	+1	0	0	0	0	0	0	0	0	0	0	0	0	0	0	0	0	0	0
	0	0	-1	0	0	0	0	0	0	0	0	0	0	0	0	0	+1	0	0	0	0	0	0
	0	0	0	-1	0	0	0	0	0	0	0	0	0	0	0	0	0	+1	0	0	0	0	0
	0	0	0	0	-1	0	0	0	0	0	0	0	0	0	0	0	0	+1	0	0	0	0	0
	0	0	0	0	0	+1	0	0	0	0	0	0	0	0	0	0	-1	0	0	0	0	0	0
	0	0	0	0	0	0	+1	0	0	0	0	0	0	0	0	0	0	-1	0	0	0	0	0
	0	0	0	0	0	0	0	+1	0	0	0	0	0	0	0	0	0	0	-1	0	0	0	0
	0	0	0	0	0	0	0	0	-1	0	0	0	0	0	0	0	0	0	0	+1	0	0	0
	0	0	0	0	0	0	0	0	0	0	0	-1	0	0	0	0	0	0	0	0	0	+1	0
	0	0	0	0	0	0	0	0	0	0	0	0	+1	0	0	0	0	0	0	0	-1	0	0
	0	0	0	0	0	0	0	0	0	0	0	0	0	+1	0	0	0	0	0	0	0	0	-1
	0	0	0	0	0	-1	-1	-1	0	0	0	0	0	0	0	+1	0	0	0	0	0	0	0
	0	0	0	0	0	0	0	0	+1	+1	+1	0	0	0	-1	0	0	0	0	0	0	0	0
	0	+1	0	0	0	0	0	0	0	0	0	0	-1	-1	-1	0	0	0	0	0	0	0	0
	0	-1	0	0	0	0	0	0	0	0	0	0	0	0	0	0	0	0	0	0	0	0	0

Figure 4. Node-arc incidence matrix A.

Table 4. Pressure of Natural Gas at All of the Nodes of the Pipeline Network

Node	Pressure (bar)	Node	Pressure (bar)	Node	Pressure (bar)
0	61.200	6	66.919	12	65.510
1	47.359	7	67.030	13	65.186
2	47.042	8	58.324	14	66.809
3	47.122	9	58.260	15	58.386
4	47.192	10	58.354	16	65.072
5	67.018	11	65.185	17	58.800

Analysis Sensitivity. Like any NLP solver, CONOPT gives the Lagrange parameters representing the shadow prices for constraints or the reduced costs for variables. All these parameters are null or quasi-null except for the supply pressure at Node 0 (value = -0.047), the delivery pressure at Node 17 (value 0.017) and the pipeline delivery throughput fixed at 150 kg/s in arc G2 (value 0.014). This means, for example, that if the supply pressure is increased by 1 bar, the total fuel consumption will be decreased of 0.047 kg/s. In the same way, if the delivery pressure is decreased by 1 bar, the total fuel consumption will be decreased of 0.017 kg/s.

Second numerical example: multisupply multidelivery transmission network (MINLP problem)

Network Characteristics Case study 2 was provided by the French Company GdF Suez and is inspired from real data. The multisupply multidelivery transmission network is presented schematically in Figure 5. The combinatorial aspect of this example is more complex than case study 1, namely, because of the existence of three loops and seven compressor stations. The system is composed of 19 delivery points at which gas comes out from the network. These delivery points are symbolized by small empty circles. Gas can be supplied from six points (symbolized by hexagons). Moreover, 20 intermediate nodes are considered to provide necessary interconnections or, in some cases, to specify explicitly some changes in design parameters: for example, Node 103 is defined to introduce the effect of diameter change between arcs 0100 and 0090 in the model. For the same purpose, Node 66 is introduced because the pressure limits are different at the endpoints of its neighboring arcs. The oblong shape between Nodes 59 and 152 indicates that two pipes of same length, but with different diameters and roughness (0000 and 0880) are installed between these two nodes. Globally, the network consists of 45 nodes and 30 pipe arcs. In addition, seven compressors are located to com-

Table 5. Optimal Values of the Flow Rate for Each Pipeline

Arc	Flow Rate (kg/s)	Arc	Flow Rate (kg/s)	Arc	Flow Rate (kg/s)
G1	150.750	G6	49.186	G11	50.343
G2	150	G7	50.450	G12	50.200
G3	49.367	G8	50.559	G13	49.521
G4	50.637	G9	50.264	G14	50.279
G5	50.746	G10	49.587	G15	150.195

pensate pressure losses through the network. Ten valves permit to break the pressure between some pairs of points to balance the network. In some cases, a valve or more can be positioned after a compressor to regulate the output pressure of two or more streams that originate from the discharge side of compressor.

Natural gas flowing through the network is assumed to contain 91% methane and 9% ethane. Its properties are summarized in Table 7. Once more, isothermal conditions are considered in the optimization framework. In the great majority of published works, the isothermal assumption is used. From Osiadacz and Chaczykowski,⁴⁸ there is a significant difference about the pressure distribution into a pipeline network between transient and stationary behaviors. In the steady-state case, as the compression processes reduce the gas temperature, the increase of gas temperature along the pipes is counter-balanced. So from a global point of view, a steady-state network can be considered as isothermal.

The principal characteristics of pipe arcs including their length, internal diameter, and inner surface roughness, as well as maximum admissible operating pressure, are displayed in Table 8. The pressure bounds that have to be respected for each node are presented in Table 9. The pressure of the supply node 114 should be considered invariable at 85 bars, value prefixed by the gas supplier. Therefore, these lower and upper bounds are set at this pressure. Gas consumption flow rates at delivery nodes are set at the values given in Table 10. These amounts should be guaranteed for the different customers. From the point of view of flow rates, the most important delivery nodes are 99, 89, 95, and 9, respectively. Besides, from the pressure standpoint, a more elevated pressure value must be respected at Node 99, which explains the important value of the lower bound (61) of Table 9. Delivery gases are provided from six supply nodes situated on the network. The maximum gas flow rate demands from each supply node are presented in Table 11. The principal supply nodes are Nodes 110 and 114. If design or operational constraints allow it, these two nodes are able to satisfy 75% of gas demands.

Table 6. Optimal Values of Discharge Flow Rate, Rotational Speed, Fuel Consumption, Isentropic Head, and Isentropic Efficiency for the Compressor Units of the Network

Compressor	C1	C2	C3	C4	C5	C6
Discharge flow rate (kg/s)	49.186	50.450	50.559	50.200	49.521	50.279
Rotational speed (rpm)	244.348	246.482	246.558	166.7	166.7	166.7
Fuel consumption (kg/s)	0.182	0.186	0.187	0.064	0.066	0.064
Consumption ratio (%)	0.369	0.367	0.369	0.127	0.133	0.127
Isentropic head (kJ/kg)	42.592	42.188	42.201	12.664	13.367	12.607
Isentropic efficiency (%)	74.917	74.215	74.207	64.195	65.331	64.101

Table 7. Characteristics of Natural Gas in Case Study 2

Higher heating value (HLV) (kJ/m ³)	4.18 × 10 ⁴
Specific gravity in relation to air	0.6
Gas temperature (K)	278.15
Heat capacity ratio	1.309
Assumed composition	Methane: 91%, ethane: 9%

MINLP Formulation. To tackle the problem, flow directions for each pipe arc as well as for each compressor and valve arc are not imposed in advance. Let us note that some arc directions are considered to be imposed without ambiguity during the optimization process. They consist of the following elements: pipes 0051, 0060, 0110, 0150, 0170, 0240, 0290, 0340, 0390, 0920, 0930, 1050, compressors C5 and C6, valves V1 and V6 as shown by the arrows in Figure 5. For each other arc a binary variable d_i is assigned to identify its flow direction. This binary can be 0 or 1: when it is equal to 0, the gas flows in the arc opposite to the preliminary direction which is the direction conform to the corresponding node-arc incidence matrix. The mixed integer nonlinear problem is formulated below.

The continuous variables are pressures at nodes and flow rates corresponding to pipes, valves, and compressors in addition to the gas injection flow rates at supply nodes. They all take positive values. There are 44 pressures at nodes without taking into account the pressure subjected to the node 114 that is fixed at 85 bar. The total number of flow rates corresponding to arcs and the total number of the sup-

Table 8. Principal Characteristics of Pipe Arcs

Pipe Arc	Length (km)	Diameter (mm)	MAOP (bar)	Roughness (μm)
0000	64.1	754	68	20
0010	101.6	688	68	20
0020	80.4	681	68	10
0030	27.1	617	68	10
0051	172.699	1090	85	10
0060	4.9	1167	68	10
0080	122.2	1069	68	10
0090	41.6	1069	68	10
0100	28.4	1054	68	10
0110	81.3	895	68	10
0150	21.6	874	68	10
0160	14.2	954	68	10
0170	46.8	595	68	10
0200	43.3	948	68	10
0240	27.9	588	56.8	10
0260	95.701	744	68	10
0280	119.715	744	68	10
0290	4.9	892	80	10
0300	30.9	1167	80	10
0310	53.4	892	80	10
0321	54.5	892	68	10
0331	77	892	68	10
0340	89.0	794	68	10
0390	63.9	493	68	20
0880	64.1	994	68	10
0900	204.5	994	68	10
0910	36.2	994	68	10
0920	125.8	891	85	10
0930	67.7	891	85	10
1050	0.001	1000	68.7	10

Table 9. Bounds on Node Pressures

Node	Pressure Lower Bound (bar)	Pressure Upper Bound (bar)	Node	Pressure Lower Bound (bar)	Pressure Upper Bound (bar)
29	40	86	105	40	56.8
30	40	86	110	40	67
62	40	49	114	85	85
66	40	86	119	40	81
76	40	81	141	60	86
98	40	81	144	40	56.8
99	61	86	Other	40	68.7

ply flow rate variables are 47 and 6, respectively. As mentioned earlier, a total number of 47 binary variables are introduced for flow direction of arcs. Because of the problem definition, fixed flow directions are assumed for some arcs (for instance arc 0051 where the gas flows always from the supply node 114 towards the node 141) so that the real number of binary variables is finally reduced to 31. Altogether, there are 31 binary variables and 97 continuous variables.

The constraints (equality, inequality, mixed) are defined in section Problem formulation. There are 45 material balances around nodes, 30 equations of motion for pipes, seven equations to express compressor pressure ratios, and seven other equations to calculate fuel rate consumptions. Ten mixed linear inequalities (Eq. 31) related to the valves, complete this set of constraints. The objective function is expressed by Eq. 34.

Problem Solution. The problem is solved by using the SBB solver and CONOPT is implemented for solving NLP subproblems. The optimum results are dependent on the initial assumed values of flow directions in arcs, due to the presence of local optima.

Mainly due to the complexity (for instance, nonlinearities) involved in the MINLP models, good initial values and bounds are essential to achieve convergence toward a local optimum. The selected initialization scheme lies on the generation of a set of binary variables provided by the user, whereas the continuous variables are automatically initialized by the solver because they are well bounded and scaled. Five initializations configurations of binary variables referred as Cases 1 to 5 were selected.

(1) In Case 1, all the binary variables are initially chosen equal to one, except that of pipeline 0030. Consequently, the

Table 10. Amount of Gas Consumptions Delivered by the Pipeline Network

Node	Delivery Gas (kg/s)	Node	Delivery Gas (kg/s)
7	16.15	87	42.064
9	119.988	89	146.964
11	42.596	94	19.987
19	20.436	95	126.622
23	36.824	98	73.574
29	6.866	99	172.76
55	41.693	102	0.393
59	63.628	105	23.011
60	59.507	154	75.678
82	62.274	Total	1 151.014

Table 11. Maximum Rate of the Gas Provided from the Supply Nodes

Node	Maximum Rate (kg/s)	Node	Maximum Rate (kg/s)
62	78.406	114	400.564
76	190.786	210	53.377
110	474.331	214	68.652

binary variable corresponding to valve V7 is also equal to zero.

(2) In Case 2, the independent binary with a zero value is only that of pipeline 0010 and its associated compressor C1.

(3) In Case 3, a zero value is attributed to the binary value corresponding to pipeline 0280 and to the related valve V8.

(4) In Case 4, a zero value is assigned to the binary variables related to pipelines 0010, 0030, 0260, and 0321. Consequently, in this case, the binaries related to compressors C1, C2, C3 and the valve V7 are also equal to zero.

(5) Finally, in the most dispersed situation that is Case 5, the binaries corresponding to pipelines 0010, 0030, 0260, 0321, 0910 and that of compressor C4 are set initially at zero, which also leads to the same value for dependent binaries related to compressors C1, C2, C3, and C7 as well as to valve V7.

For all the initial points, the initial value of the total fuel consumption is 0.999 kg/s and the resolution requires about 3 s CPU on the same PC and with the same tolerances as above. It was observed that, with these initial guess schemes, the same structure is always obtained (compressors C4 and C7) but two sets of operating conditions were found. To guarantee gas flow in the network without violation of any constraint, the results show that compressors C4 and C7 work with different power consumptions. The values of the different variables related to these two stations are shown in Table 13 for all solution points. It has been verified that none of the values presented in this table hits one of its bound. Note that the other compressors are bypassed.

Besides, in these study cases, no gas flows through pipeline 0030, valves V2 and V7 whereas valve V5 is totally open. Let us note that only for initialization Cases 1 and 4, valve V8 is also totally open. This result is obtained by comparing the end-point pressures of each valve.

Table 12. Principal Characteristics of the Compressors

Compressor	MAOP (bar)	Capacity, Standard (m ³ /hr)	Maximum Pressure Ratio	Maximum Power (MW)
1	80	5.60×10^5	1.35	3.9
2	80	1.75×10^6	1.50	17.6
3	80	7.50×10^5	1.34	5.3
4	80	9.60×10^5	1.39	9.4
5	80	2.40×10^6	1.46	34
6	80	1.36×10^6	1.56	14
7	86	9.50×10^5	1.90	22

Using Case 2 as an initialization scheme, it was found that all binary variables are equal to unity that means that all flow directions are the same. Yet in the optimal structure, there is no gas flow in pipeline 00280 as well as through valves V2 and V8. In addition, valves V3, V9, and V10 are totally open. In Case 3 (see Table 14), the calculations give a zero value for gas flow rate through valve V2 at the optimal solution and valves V4, V5, V7, V8, and V10 are totally open. The best solution for the problem is obtained using Case 3 as an initialization guess: the value of objective function is 0.370 kg/s, which is very near from the value obtained for Case 2. Having a look at Table 9, it is observed that the pressures at delivery Nodes 99 and 105 are obtained at their lower bounds. In the same time, the pressures of supply Nodes 62 and 110 are calculated to be at their upper limits: with this operating mode, the number of compressors is minimized and the compressors that are in operation consume smaller amounts of energy. Consequently, the value of objective function is reduced. Table 15 presents the flow rates of each arc for the best optimum solution (Case 3) where Valve 2 is closed. It can be noted that compared with the initial solution (0.999 kg/s), the optimal value of Case 3 (0.370 kg/s) represents a gain of 68%.

Flow directions in arcs for the best optimal point are outlined in Figure 6. In addition, pressures subjected to nodes for this solution are reported in Figure 7. This optimal solution is outlined in Figure 8. Comparing end-point pressures of each valve, it can be deduced that valves 1, 3, 6, and 9 are only partially open. Only these valves are displayed in Figure 8. Note that all valves are presented in Figures 6 and 7; however, they must be completely open or closed. In

Table 13. Operating Conditions of the Compressors in Work Obtained by MINLP Using Different Initialization for Flow Direction in Arcs

Case	Compressor	Pressure Ratio	Input Pressure (bar)	Throughput (kg/s)	Power Consumption (kW)	Fuel Consumption (kg/s)	
1, 4	C4	1.102	44.180	139.186	6090	0.111	
	C7	1.262	57.155	179.946	17587	0.320	
Total (objective function):							0.431
2	C4	1.065	45.680	106.03	3013	0.055	
	C7	1.262	57.170	179.945	17567	0.320	
Total (objective function):							0.375
3	C4	1.062	45.822	102.239	2761	0.050	
	C7	1.262	57.177	179.945	17557	0.320	
Total (objective function):							0.370
5	C4	1.102	44.179	139.295	6010	0.109	
	C7	1.263	57.156	179.946	17586	0.320	
Total (objective function):							0.430

Table 14. Pressure at Diverse Nodes of the Transmission Network According to the Best Optimum Solution Obtained by MINLP Method (Case 3)

Node	Pressure (bar)	Node	Pressure (bar)	Node	Pressure (bar)
7	53.364	59	65.562	105	40
8	53.364	60	45.041	110	67
9	44.275	62	49	111	48.961
10	44.275	65	54.71	114	85
11	40	66	65.178	119	46.501
19	40.976	76	47.332	121	42.949
20	40.976	82	54.324	140	54.324
23	45.822	87	40	141	69.17
24	48.671	89	47.619	144	40.441
29	72.175	94	41.206	145	44.275
30	57.177	95	51.053	148	40.991
49	66.596	98	46.813	152	66.596
50	66.596	99	61	154	48.961
55	40.991	102	58.705	210	44.275
56	40.991	103	51.311	214	52.452

addition, the bypassed compressors for which pressure ratios are equal to one are shown in the latter figure, but there is no gas consumption in them. Finally, Table 16 presents the flow rates corresponding to each supply node. Comparing these operational supply rates with Table 11, it can be noted that all nodes are used with their maximum supply rates except for Nodes 62 and 110. Having a look at Table 10, it is observed that the totality of the supply gases is equal to the summation of the delivery gases and gas consumption in the compressor stations.

Analysis Sensitivity. As in the previous example, a sensitivity analysis was carried out for the five cases, but only the study related to Case 3 is reported here. The other cases provide similar results. All the Lagrange parameters are null or quasi-null except for the supply pressure at Node 110 (value = -0.033), the supply pressure at Node 62 (value = -0.020), the delivery pressure at Node 99 (value = 0.015), the delivery pressure at Node 11 (value = 0.014), the gas flow rate in valve 2 (value = 0.003), and the delivery pressure at Node 87 (value = 0.002).

For the supply Nodes 76, 210, and 214, the solution is found between the bounds, and the Lagrange multipliers

are null. For the supply Node 114, the pressure is fixed at 85 bars, and the Lagrange multiplier is also zero. The solution for the supply Nodes 110 and 62 is on the upper bound, leading to non-null parameters. For example, if the supply pressure is increased of 1 bar at node 110, the total fuel consumption will be decreased of 0.033 kg/s.

For the internal delivery Nodes 7, 9, 19, 23, 29, 55, 59, 60, 82, 89, 94, 95, 98, 102, and 154 the optimizer finds a solution between the bounds, leading to null Lagrange parameters. For the four terminal delivery Nodes 11, 87, 99, and 105, the optimal solution is on the lower bound, giving non-null multipliers (for Node 105 the multiplier is very low). For example if the delivery pressure at Node 99 is decreased of 1 bar, the total fuel consumption will be decreased of 0.015 kg/s.

About the Bilinear Constraint (33). For each valve of the network, the constraint (33) expresses that the output pressure must be less than the input one. Insofar as in the considered example, the flow direction is not known and represented by a binary variable d_j , constraints (33) involve products between pressures (p_i) and directions,

Table 15. Flow Rate Through Pipes, Compressors, and Valves Obtained by MINLP (Case 3)

Arc	Flow Rate (kg/s)	Arc	Flow Rate (kg/s)	Arc	Flow Rate (kg/s)
0000	55.758	0280	3.791	C3	16.645
0010	112.604	0290	190.786	C4	102.239
0020	96.454	0300	117.212	C5	413.802
0030	36.947	0310	117.212	C6	42.064
0051	400.564	0321	87.548	C7	179.945
0060	413.802	0331	87.548	V1	23.011
0080	57.233	0340	42.064	V2	0
0090	268.902	0390	42.596	V3	57.233
0100	268.902	0880	120.473	V4	176.231
0110	126.622	0900	180.338	V5	268.902
0150	24.202	0910	179.945	V6	400.564
0160	217.426	0920	172.76	V7	36.947
0170	68.652	0930	172.76	V8	3.791
0200	139.113	1050	53.377	V9	36.632
0240	23.011	C1	112.604	V10	211.669
0260	16.645	C2	87.548		

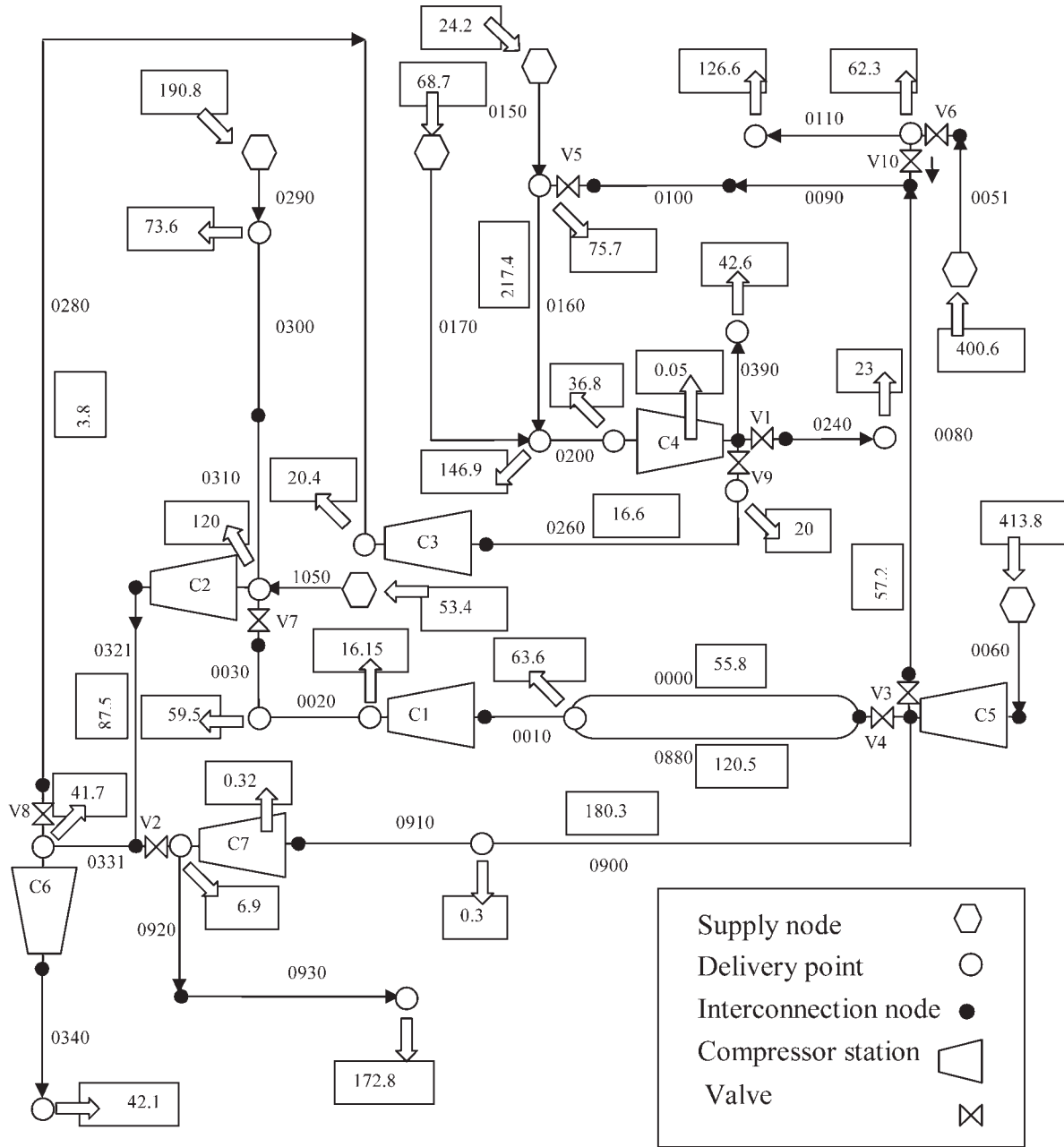


Figure 6. Flow sheet of the best solution obtained by MINLP (Case 3).

Note: flow rates are reported in the cubes.

inducing bilinearities in the search space defined by the set of constraints. It is well-known that bilinearities give birth to nonconvex regions, and consequently to convergence difficulties. For avoiding bilinearities, the following formulation (Eqs. 33a, 33b, 33c, and 33d) is proposed:

$$\sum_i a_{ij} p_i^1 - a_{ij} p_i^2 \geq 0 \quad j \in N_v \quad i \in N_n \quad (33a)$$

$$0 \leq p_i^1 \leq U_{pi} d_j \quad j \in N_v \quad i \in N_n \quad (33b)$$

$$0 \leq p_i^2 \leq U_{pi}(1 - d_j) \quad j \in N_v \quad i \in N_n \quad (33c)$$

$$p_i^1 + p_i^2 = p_i \quad i \in N_n \quad (33d)$$

The term U_{pi} is the upper bound on pressures ($U_{pi} = 100$ bar), p_i^1 and p_i^2 are new variables added.

The problem was solved again with this new formulation, for the five initializations corresponding to Cases 1 to 5. For Case 3, the solution reported in Table 13 is obtained (objective function = 0.370 kg/s). For Cases 1, 2, 4, and 5, the

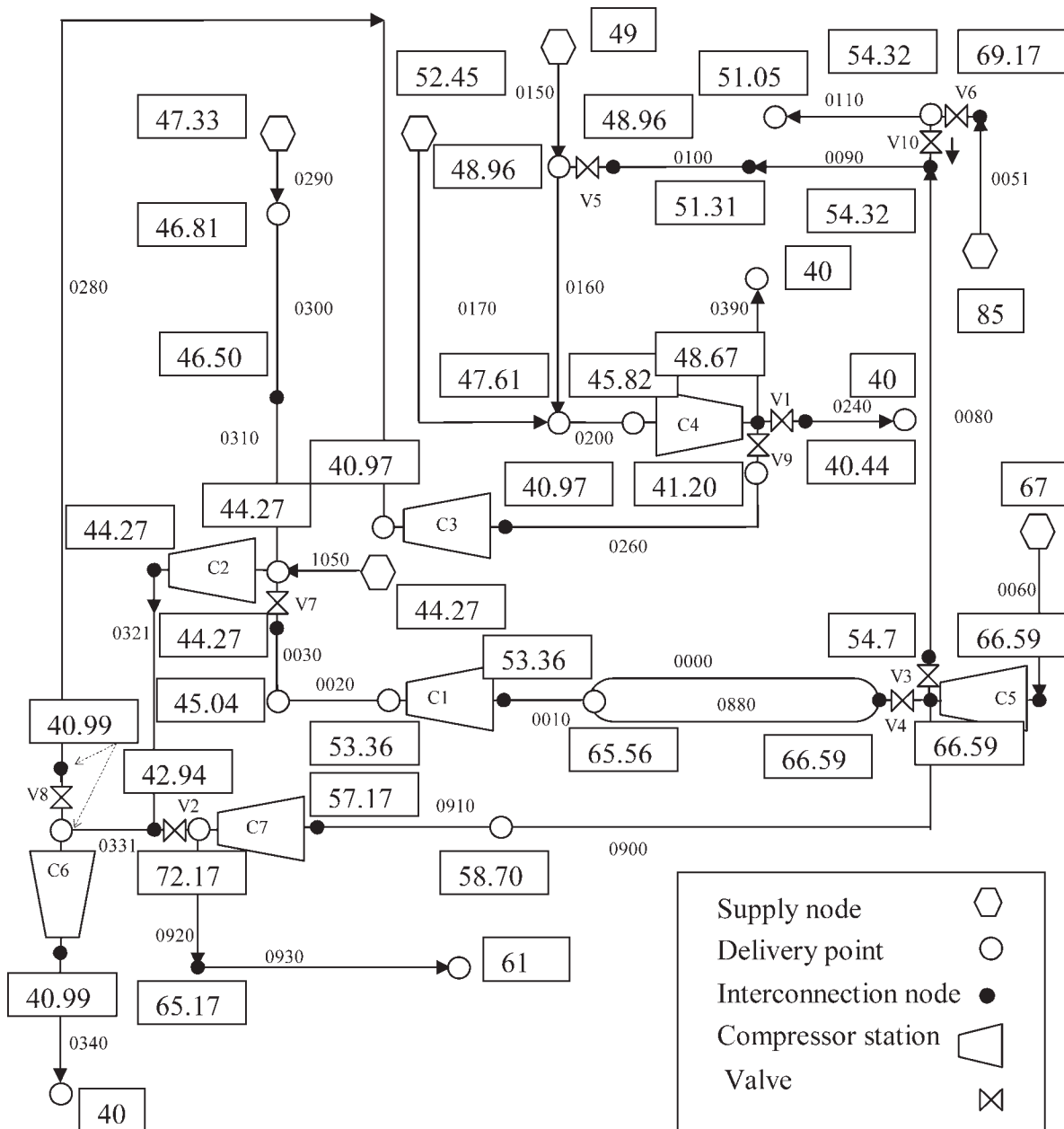


Figure 7. Flow sheet of the best solution obtained by MINLP with pressures (Case 3).

Note: pressures are reported in the cubes.

same solution as in Case 3 is found again. In conclusion, the reformulation of the bilinear constraint (33) allows reaching a single solution (global optimum), instead of four local solution as reported in Table 13.

Conclusions

The use of the objective function related to the improvement of operating conditions of a gas network under fuel consumption minimization is particularly interesting as reduction of the energy used in pipeline operations will have a significant economical impact. The proposed strategy can help the gas network manager to answer these recurrent questions:

- Knowing that I need to deliver a certain volume of gas at certain key points, how do I utilize the compressors at my disposal most efficiently to reduce fuel gas consumption?

- How do I set the consequent pressures and flow rates?

In this study, characteristic values for compressor stations of some key parameters that may be useful for the practitioner (isentropic head, isentropic efficiency...) are systematically computed. The modeling gas pipeline networks including gas pipeline equations, maximum allowable operational pressure, critical velocities, compressor characteristics, and network representation by using incidence matrices are detailed in the work of Tabkhi.⁴⁹

Before presenting the examples, the MINLP problem is established from the definition of the optimization variables,

rotational speeds and can yield significant reductions in the fuel consumption. A sensitivity analysis based on the shadow prices and reduced costs shows that the most sensitive variables are the pressures at supply points, followed by the pressures at terminal delivery points. For the most complex example, several local solutions are found, depending on initial guesses. However, when substituting the bilinear constraint by an equivalent linear formulation, the same solution (global optimum) is found, whatever the initial guess.

The framework proposed here can help the decision maker for optimizing the operating conditions of gas networks and anticipating the changes that may occur, i.e., gas quality, variation in supply sources availability and consequences in maintenance.

Acknowledgments

The authors would like to thank Jean André (GdF Suez) for fruitful discussions and for the “big size” example illustrating the proposed methodology.

Literature Cited

- Riva A, D'Angelosante S, Trebeschi C. Natural gas and the environmental results of lifecycle assessment. *Energy*. 2006;31:138–148.
- Suming W, Rios-Mercado RZ, Boyd EA, Scott LR. Model relaxations for the fuel cost minimization of steady-state gas pipeline networks. *Math Comput Model*. 2000;31:197–220.
- Tian S, Adewumi MA. Development of analytical design equation for gas pipelines. *SPE Prod Facil*. 1994;9:100–106.
- Lewandowski A. Object-oriented modelling of the natural gas pipeline network. *Proceedings of the 26th Annual Meeting of Pipeline Simulation Interest Group*, San Diego, 1994.
- Osiadacz AJ. Dynamic optimization of high Pressure gas Networks using hierarchical systems theory. *Proceedings of the 26th Annual Meeting of Pipeline Simulation Interest Group*, San Diego, 1994.
- Surry PD, Radcliffe NJ, Boyd ID. A multi-objective approach to constrained optimization of gas supply networks. In: Fogarty T. C., ed. *The COMOGA Method, Lecture Notes in Computer Science, Evolutionary Computing*. Berlin/Heidelberg: Springer, 1995:166–180.
- Mohitpour M, Thompson W, Asante B. The importance of dynamic simulation on the design and optimization of pipeline transmission systems. *Proc ASME Int Pipeline Conf*. 1996;2:1183–1188.
- Boyd EA, Scott LR, Wu SS. Evaluating the quality of pipeline optimization algorithms. *Proceedings of the 29th Annual Meeting of Pipeline Simulation Interest Group*, Tucson, 1997.
- Costa ALH, de Medeiros JL, Pessoa FLP. Steady-state modelling and simulation of pipeline networks for compressible fluids. *Braz J Chem Eng*. 1998;15:344–357.
- Sung W. Optimization of pipeline networks with a hybrid MCST-CD networking model. *SPE Prod Facil*. 1998;13:213–219.
- Sun CK, Varanon U, Chan CW, Tontiwachwuthikul P. An integrated expert system/operations research approach for optimization of natural gas pipeline operations. *Eng Appl Artif Intell*. 1999;13:465–475.
- Rios-Mercado RZ, Wu S, Scott LR, Boyd EA. A reduction technique for natural gas transmission network optimization problems. *Ann Oper Res*. 2001;117:217–234.
- Martinez-Romero N, Osorio-Peralta O, Santan-Vite I. Natural gas network optimization and sensibility analysis. *Proceedings of the SPE International Petroleum Conference and Exhibition*, Villahermosa, Mexico, 2002:357–370.
- Cobos-Zaleta D, Rios-Mercado RZ. A MINLP model for minimizing fuel consumption on natural gas pipeline networks. *XI Latin-Ibero-American Conference on Operations Research*, Concepción Chile, 2002.
- Mora T, Ulieru M. Minimization of energy use in pipeline operations—an application to natural gas transmission systems. *Industrial Electronics Society, IECON, 31st Annual Conference of IEEE*, Raleigh, NC, 2005. ISBN: 0-7803-9252-3.
- Chauvelier-Alario M, Mathieu B, Toussaint C. Decision making software for Gaz de France distribution network operators. *Carpathe, 23rd World Gas Conference*, Amsterdam, Netherlands, 2006.
- André J, Bonnans F, Cornibert L. Planning reinforcement on gas transportation networks with optimization methods. *Process Operation Research Models and Methods in the Energy Sector Conference, ORMMES*, Coimbra, Portugal, 2006.
- Wolpert DH, Macready WG. No free lunch theorems for optimization. *IEEE Trans Evol Comput*. 1997;1:67–82.
- Hao J, Galinier P, Habib M. Métaheuristiques pour l'optimisation combinatoire et l'affectation sous contrainte. *Revue d'intell Artif*. 1999;13:283–324.
- Grossmann IE. Review of nonlinear mixed-integer and disjunctive programming techniques. *Optim Eng*. 2002;3:227–252.
- Biegler LT, Grossmann IE. Retrospective on optimization. *Comput Chem Eng*. 2004;28:1169.
- Ponsich A. *Stratégies d'Optimisation Mixte en Génie des Procédés—Application à la Conception d'Ateliers Discontinus*, PhD Thesis. France: Institut National Polytechnique de Toulouse, 2005.
- Duran MA, Grossmann IE. An outer-approximation algorithm for a class of mixed-integer nonlinear programs. *Math Program*. 1986;36:307–339.
- Gupta OK, Ravindran V. Branch and bound experiments in convex nonlinear integer programming. *Manag Sci*. 1985;31:1533–1546.
- Ryoo HS, Sahinidis NV. Global optimization of nonconvex NLPs and MINLPs with applications in process design. *Comput Chem Eng*. 1995;19:551–566.
- Smith EMB, Pantelides CC. A symbolic reformulation/spatial branch-and-bound algorithm for the global optimization of nonconvex MINLPs. *Comput Chem Eng*. 1999;23:457–478.
- Geoffrion AM. Generalized benders decomposition. *J Optim Theory Appl*. 1972;10:237–260.
- Westerlünd T, Petterson F. An extended cutting plane method for solving convex MINLP problems. *Comput Chem Eng*. 1995;19:S131–S136.
- Raman R, Grossmann IE. Modeling and computational techniques for logic based integer programming. *Comput Chem Eng*. 1995;18:563–578.
- Brooke A, Kendrick D, Meeraus A, Raman R. *GAMS: A User's Guide*. Washington: GAMS Development Corporation, 2004.
- Leyffer S. User manual for MINLP_BB, University of Dundee. Numerical Analysis Report NA/XXX. 1999.
- Westerlünd T, Lundqvist K. *Alpha-ECp, version 5.04*. An Interactive MINLP-Solver Based on the Extended Cutting Plane Method. Report 01–178-A. *Process Design Laboratory*. Finland: Abo Akademi University, 2003.
- Kearfoot RB. Interval analysis: interval Newton method. *Encyclopedia Optimization*. 2001;3:76–78.
- Csendes T. Generalized subinterval violation criteria for interval global optimization. *Numerical Algorithms*. 2004;37:93–100.
- Kirkpatrick S, Gelatt JCD, Vecchi MP. Optimization by simulated annealing. *IBM Research Report*, RC9355. 1982.
- Teh YS, Rangaiah GP. Tabu search for global optimization of continuous functions with application to phase equilibrium calculations. *Comput Chem Eng*. 2003;27:1665–1679.
- Holland JH. *Adaptation in Natural and Artificial Systems*. MI: University of Michigan Press, 1975.
- Beyer HG, Schwefel HP. Evolution strategies, a comprehensive introduction. *Nat Comput*. 2002;1:3–52.
- Yang YW, Xu JF, Soh CK. An evolutionary programming algorithm for continuous global optimization. *Eur J Oper Res*. 2006;168:354–369.
- Romeo E, Royo C, Monzon A. Improved explicit equations for estimation of the friction factor in rough and smooth pipes. *Chem Eng J*. 2002;86:369–374.
- Mohring J, Hoffmann J, Halfmann T, Zemitis A, Basso G, Lagoni P. Automated model reduction of complex gas pipeline networks. *Proceedings of the 36th Annual Meeting of Pipeline Simulation Interest Group*, Palm Springs, California, 2004.
- Menon ES. *Gas Pipeline Hydraulics*. Boca Raton: CRC Press, Taylor and Francis Group, 2005.

43. Smith JM, Van Ness HC. *Introduction to Chemical Engineering Thermodynamics*, 4th ed. Singapore: McGraw-Hill Book Company, 1998.
44. Abbaspour M, Chapman KS, Krishnaswami P. Nonisothermal compressor station optimization. *J Energy Resour Technol.* 2005;127: 131–141.
45. Odom FM. Tutorials on modelling of gas turbine driven centrifugal compressors. *Proceedings of the 22nd Annual Meeting of Pipeline Simulation Interest Group*, Baltimore, Maryland, 1990.
46. Pagnet JM. Pompage des compresseurs, Techniques de l'ingénieur. *Génie Mécanique.* 1999;BL2:BM4182.1–BM4182.18.
47. Gorla RSR, Khan AA. *Turbomachinery Design and Theory*. New-York: Marcel Dekker, 2003.
48. Osiadacz AJ, Chaczykowski M. Comparison of isothermal and non-isothermal pipeline gas flow models. *Chem Eng J.* 2001;81: 41–51.
49. Tabkhi F. *Optimisation de Réseaux de Transport de Gaz*, PhD Thesis. Institut National Polytechnique de Toulouse, France. 2007.